^{68}Ga-Pentixafor PET/CT for Imaging of Chemokine Receptor 4 Expression in Waldenström Macroglobulinemia/Lymphoplasmacytic Lymphoma: Comparison to ^{18}F-FDG PET/CT

Yaping Luo*[1,2], Xinxin Cao*[3], Qingqing Pan[1,2], Jian Li[3], Jun Feng[3], and Fang Li[1,2]

[1]Department of Nuclear Medicine, Chinese Academy of Medical Sciences and Peking Union Medical College Hospital, Beijing, People's Republic of China; [2]Beijing Key Laboratory of Molecular Targeted Diagnosis and Therapy in Nuclear Medicine, Beijing, People's Republic of China; and [3]Department of Hematology, Chinese Academy of Medical Sciences and Peking Union Medical College Hospital, Beijing, People's Republic of China

^{18}F-FDG PET/CT has some limitations in the evaluation of Waldenström macroglobulinemia/lymphoplasmacytic lymphoma (WM/LPL), an indolent B-cell lymphoma that primarily involves the bone marrow. Because there is a high level of chemokine receptor 4 expression in the B cells of WM/LPL patients, we performed a prospective cohort study to evaluate the performance of ^{68}Ga-pentixafor, which targets chemokine receptor 4 in WM/LPL, and to compare it with the performance of ^{18}F-FDG. **Methods:** Seventeen patients with WM/LPL were recruited. All patients underwent both ^{68}Ga-pentixafor PET/CT and ^{18}F-FDG PET/CT. A positive PET/CT result was defined as the presence of focal lesions with positive PET results or diffuse bone marrow patterns (uptake > liver). The rates of positive results for PET/CT scans of bone marrow, lymph nodes, and other extramedullary involvement were statistically compared. **Results:** ^{68}Ga-pentixafor PET/CT had a higher rate of positive results than ^{18}F-FDG PET/CT (100% vs. 58.8%; $P = 0.023$) in the recruited WM/LPL patients. The sensitivities of ^{68}Ga-pentixafor PET/CT and ^{18}F-FDG PET/CT for detecting bone marrow involvement were 94.1% and 58.8%, respectively ($P = 0.077$). In terms of detecting lymph node involvement, ^{68}Ga-pentixafor PET/CT had a significantly higher rate of positive results than ^{18}F-FDG PET/CT (76.5% vs. 11.8%; $P = 0.003$). In addition, ^{68}Ga-pentixafor detected more paramedullary and central nervous system involvement than ^{18}F-FDG. **Conclusion:** ^{68}Ga-pentixafor might be a promising imaging agent for the assessment of WM/LPL.

Key Words: Waldenström macroglobulinemia; lymphoplasmacytic lymphoma; CXCR4; ^{68}Ga-pentixafor; PET/CT

J Nucl Med 2019; 60:1724–1729
DOI: 10.2967/jnumed.119.226134

Waldenström macroglobulinemia/lymphoplasmacytic lymphoma (WM/LPL) is an uncommon indolent non-Hodgkin lymphoma characterized by the accumulation of lymphoplasmacytic cells in the bone marrow and the excess production of monoclonal immunoglobulin. ^{18}F-FDG PET/CT, a standard technique in the diagnosis and management of several types of tumors, has a limited role in diagnosing WM/LPL. According to the consensus recommendations of the International Conference on Malignant Lymphoma, ^{18}F-FDG PET/CT is recommended for the routine staging of ^{18}F-FDG–avid nodal lymphomas and is the gold standard for essentially all histologies; however, it is not indicated for WM/LPL, unless there is a suspicion of aggressive transformation (*1*). Data on the use of ^{18}F-FDG PET/CT in WM/LPL are very limited. A study on the role of ^{18}F-FDG PET/CT imaging in WM showed that only 43% of patients had abnormal bone marrow uptake (*2*), despite bone marrow being the primary site of involvement.

Chemokine receptor 4 (CXCR4) is a key factor for tumor growth and metastasis and is expressed at a high density in at least 20 different types of solid cancers and hematopoietic malignancies (*3*). ^{68}Ga-pentixafor, a novel PET tracer with a high affinity for CXCR4, was recently introduced for the assessment of several lymphoproliferative diseases, such as multiple myeloma, diffuse large B-cell lymphoma, and acute myeloid leukemia (*4–7*). Studies have shown a higher level of CXCR4 expression in the B cells of patients with WM/LPL than in the B cells of healthy donors (*8,9*); this feature makes it possible for WM/LPL to be imaged with ^{68}Ga-pentixafor. We previously reported data from a patient who had WM and in whom ^{68}Ga-pentixafor PET/CT showed intense radioactivity in the bone marrow and lymph nodes that was superior to that shown by ^{18}F-FDG PET/CT (*10*). In the present study, we aimed to further evaluate the performance of ^{68}Ga-pentixafor PET/CT in WM/LPL and to compare it with the performance of ^{18}F-FDG PET/CT, which served as a reference.

MATERIALS AND METHODS

Study Design and Patients

This is a preliminary report of an ongoing prospective study evaluating the role of ^{68}Ga-pentixafor PET/CT in WM/LPL. The study was approved by the Institutional Review Board of Peking Union Medical College Hospital (protocol ZS-1113) and was registered at ClinicalTrials.gov (NCT 03436342). To compare differences between imaging techniques, we used the rates of positive results of ^{68}Ga-pentixafor PET/CT and ^{18}F-FDG PET/CT for WM/LPL as the endpoints

Received Jan. 27, 2019; revision accepted May 7, 2019.
For correspondence or reprints contact: Fang Li, Beijing Key Laboratory of Molecular Targeted Diagnosis and Therapy in Nuclear Medicine, Wangfujing, Dongcheng District, Beijing 100730, People's Republic of China.
E-mail: lifang@pumch.cn
*Contributed equally to this work.
Published online May 17, 2019.

in this preliminary study. A total of 17 patients diagnosed with WM/LPL at the Department of Hematology, Peking Union Medical College Hospital, were consecutively recruited from April 2017 to November 2018. Written informed consent was obtained from each patient. The clinical history and laboratory test results related to WM/LPL were recorded at enrollment in the study. Patients were then referred for ^{18}F-FDG and ^{68}Ga-pentixafor PET/CT for evaluation of the disease; the scans were performed within 1 wk after enrollment. The imaging characteristics were analyzed afterward.

PET/CT Imaging

The radiolabeling of ^{68}Ga-pentixafor was performed manually immediately before injection. In brief, 45 μL of sodium acetate (1.25 M) was added to 1 mL of $^{68}GaCl_3$ eluent ($^{68}Ga^{3+}$ in 0.5 M HCl) obtained from a ^{68}Ge/^{68}Ga generator (ITG) to adjust the pH to 3.5–4.0. After the addition of a 20-μL aliquot (1 μg/μl) of DOTA-CPCR4-2 (CSBio Co.), the mixture was heated to 105°C for 15 min. The reaction solution was diluted to 5 mL and passed through a preconditioned Sep-Pak C18 Plus Light cartridge (Waters), and the cartridge was eluted with 0.5 mL of 75% ethanol to obtain the final product. The radiochemical purity of the product was analyzed by thin-layer chromatography. The ^{68}Ga-pentixafor injections were filtered through a 0.22-μm Millex-LG filter (EMD Millipore) before clinical use.

^{18}F-FDG was synthesized in-house with an 11-MeV cyclotron (CTI RDS 111).

The PET scans were performed with dedicated PET/CT scanners (Biograph 64 Truepoint TrueV [Siemens]; Polestar m660 [SinoUnion]). The PET/CT scans of 12 patients were performed with the same scanner, whereas 3 patients underwent PET/CT scans with different scanners. Two patients underwent ^{18}F-FDG PET/CT at other hospitals. For ^{18}F-FDG PET/CT, the patients fasted for at least 6 h, and the blood glucose levels were monitored (4.7–6.9 mmol/L) before an injection of ^{18}F-FDG (5.55 MBq/kg). The PET/CT images (2 min/bed) were acquired with an uptake time of 68.5 ± 12.1 (mean ± SD) min (range, 47–89 min). For ^{68}Ga-pentixafor PET/CT, imaging was performed (2–4 min/bed) with an uptake time of 47.8 ± 18.6 min (range, 30–90 min) after an injection of 84.6 ± 26.2 MBq of ^{68}Ga-pentixafor (range, 37.0–136.9 MBq). The emission scan was obtained from the tip of the skull to the midthigh. All patients underwent unenhanced low-dose CT (120 kV; 30–50 mAs) for attenuation correction and anatomic reference. The acquired data were reconstructed using the ordered-subset expectation maximization method (Biograph 64: 2 iterations, 8 subsets, gaussian filter, image size of 168 × 168; Polestar m660: 2 iterations, 10 subsets, gaussian filter, image size of 192 × 192).

Image Interpretation and Statistical Analysis

Two experienced nuclear medicine physicians visually assessed the PET/CT images and were in consensus for the image interpretation. Because WM/LPL primarily involves the bone marrow, the distribution and intensity of bone marrow uptake were regarded as the main imaging characteristics. The presence and sites of positive lymph nodes and other extramedullary involvement were also recorded. For ^{18}F-FDG, the intensity of bone marrow uptake and uptake in extramedullary lesions was based on the 5-point Deauville Scale, which is widely used for lymphoma. For ^{68}Ga-pentixafor, the intensity of involvement was classified as mild, moderate, and intense, with the liver and spleen being used as the references (mild: uptake ≤ liver; moderate: liver < uptake ≤ spleen; intense: uptake > spleen). Positive bone marrow involvement was defined as the presence of focal lesions with positive PET results (circumscribed focus of ≥5 mm with increased radioactivity compared with the background uptake in bone marrow) or diffuse bone marrow patterns (homogeneous bone marrow uptake) with the following interpretation criteria: for ^{18}F-FDG, a score of 4 for bone marrow uptake was set as a positive cutoff on the basis of the high interobserver concordance in a study of the visual descriptive criterion for multiple myeloma (*11*); and for ^{68}Ga-pentixafor, moderate or intense uptake was considered positive. The presence of positive lymph nodes and other extramedullary involvement was defined as uptake with a score of greater than or equal to 4 in ^{18}F-FDG PET and moderate or intense uptake in ^{68}Ga-pentixafor PET. The McNemar test was used to statistically compare the positive results of ^{68}Ga-pentixafor PET/CT and ^{18}F-FDG PET/CT. A P value of less than 0.05 was considered statistically significant.

RESULTS

Clinical Characteristics

Seventeen patients with WM/LPL (11 men and 6 women; 62.6 ± 10.5 [range, 48–87] y old) were enrolled in the present study. Fifteen patients had newly diagnosed WM/LPL (1 patient with smoldering WM), and 2 patients had relapsed disease (patients 3 and 5). Anemia was found in 14 of 17 patients (82.4%), and 2 of 17 patients (11.8%) had thrombocytopenia. The median proportion of infiltrated lymphoplasmacytic cells found from bone marrow aspiration was 8.75% (range, 2.5%–31.0%). Peripheral neuropathy, a common disorder induced by paraprotein in WM/LPL, was found in 3 of 17 patients (17.6%) (patients 3, 4, and 9). One patient (patient 4) had Bing–Neel syndrome (WM involving the central nervous system). Two patients (patients 6 and 11) had secondary amyloidosis due to WM/LPL. According to the International Scoring System for Waldenström Macroglobulinemia (ISS-WM) proposed in 2009 (*12*), 7 patients were classified as being at high risk and 7 patients were classified as being at intermediate risk. Two patients were classified as being at low risk. One patient with IgD κ LPL (patient 13) had an unknown risk stratification because the serum M protein and β_2-microglobulin levels were not measured; in addition, the ISS-WM may not be expanded enough to include risk stratification for IgD LPL.

Mutation of myeloid differentiation primary response 88, which has been identified in greater than 90% of WM/LPL patients by whole-genome sequencing (*13*), was documented in all patients in the present study. Three patients were found to have a CXCR4 mutation involving the C terminus that contains serine phosphorylation sites that regulate CXCR4 signaling by stromal cell–derived factor 1α (*14*). The clinical characteristics and biochemical investigations are summarized in Table 1.

Comparison of ^{68}Ga-Pentixafor and ^{18}F-FDG PET/CT

With the formerly described visual assessment criteria, ^{68}Ga-pentixafor PET/CT results were visually positive for 17 of 17 patients (100%), whereas ^{18}F-FDG PET/CT results were positive for 10 of 17 patients (58.8%). The diagnostic performance of ^{68}Ga-pentixafor PET/CT and ^{18}F-FDG PET/CT in WM/LPL is shown in Table 2.

Bone Marrow Involvement. The fact that bone marrow is the predominant site of involvement in WM/LPL was confirmed by bone marrow aspiration and biopsy in all recruited patients. According to ^{68}Ga-pentixafor and ^{18}F-FDG PET/CT, bone marrow in the spine, pelvis, and appendicular skeleton was affected in all patients; rib involvement was found in 14 patients; and 10 patients had involvement in the skull. On ^{68}Ga-pentixafor PET/CT, 10 patients had intense radioactivity in the bone marrow, with an SUV_{max} of 10.7 ± 4.1 (range, 6.0–21.3); 6 patients had moderate uptake in the bone marrow (SUV_{max}, 4.9 ± 0.8; range, 3.7–5.6). Only 1 patient had mild uptake in the bone marrow (SUV_{max}, 3.9) (classified as negative according to the visual assessment criteria in the present study); this patient had mildly elevated ^{68}Ga-pentixafor

TABLE 1
Patients' Clinical Characteristics and Biochemical Investigation Results

Patient	Age (y)	Sex	ISS-WM*	Cytogenetics†	M protein type	IgM (g/L)	M protein (g/L)	β_2-microglobulin (mg/L)	sFLC (mg/L)
1	69	M	High	$MYD88^{L265P}$	IgM λ	66.99	47.7	9.54	N/A
2	69	F	High	$MYD88^{L265P}$	IgM κ	28.93	17.5	4.85	64.7 (κ)
3	56	M	High	$MYD88^{L265P}$	IgM κ	25.32	13.1	9.28	33.8 (κ)
4	61	M	IND	$MYD88^{L265P}$	IgM κ	30.49	18.5	6.13	637.5 (κ)
5	87	M	High	$MYD88^{L265P}$	IgM κ	4.19	1.1	3.68	16.2 (κ)
6	78	F	High	MYD88 ^{L265P}	IgM κ	18.81	10.8	12.8	365.0 (κ)
7	72	M	High	$MYD88^{L265P}$	IgM κ	5.78	2.1	8.93	1,629.1 (κ)
8	56	F	IND	$MYD88^{L265P}$	IgM λ	62.43	34.3	3.06	N/A
9	72	M	IND	$MYD88^{L265P}$	IgM λ	15.2	10.5	3.27	27.2 (λ)
10	60	M	Low	$MYD88^{L265P}CXCR4^{s338x}$	IgM λ	42.91	25.3	2.34	172.5 (λ)
11	64	M	IND	$MYD88^{L265P}$	IgM λ	23.69	10.6	5.71	151.3 (λ)
12	64	M	IND	$MYD88^{L265P}$	IgM κ	53.3	32.5	5.27	159.0 (κ)
13	48	F	N/A‡	$MYD88^{L265P}CXCR4^{s338x}$	IgD κ	6.67 (IgD)§	N/A	N/A	527.5 (κ)
14	55	F	Low	$MYD88^{L265P}CXCR4^{s338x}$	IgM κ	82.49	35.6	2.93	25.7 (κ)
15	52	F	IND	$MYD88^{L265P}$	IgM κ	38.13	21.6	3.34	99.4 (κ)
16	53	M	IND	$MYD88^{L265P}$	IgM λ	20.13	13.9	3.57	89.2 (λ)
17	48	M	High	$MYD88^{L265P}$	IgM κ	77.67	47.4	6.6	6.5 (κ)

*International Staging System (ISS) for WM (ISS-WM) prognostic scoring includes age of >65 y, ß$_2$-microglobulin level of >3 mg/L, hemoglobin level of ≤11.5 g/dL, platelet count of $\leq 100 \times 10^9$/L, and IgM level of >7 g/dL. Low risk = ≤1 adverse characteristic and age of ≤65 y; high risk = ≥3 adverse characteristics; indeterminate (IND) risk = 2 adverse characteristics or age of >65 y.

†MYD88 and CXCR4 warts, hypogammaglobulinemia, infections, and myelokathexis syndrome–like somatic mutations were tested.

‡ISS-WM scoring system was not applicable (N/A) for IgD-type WM/LPL.

§Serum IgD level was measured as IgD-type M protein level.

sFLC = serum-free light chain; IND = indeterminate.

uptake in the skull, spine, pelvis, and both the proximal and the distal appendicular skeletons, including the carpals and metacarpals. With ^{18}F-FDG PET/CT, 10 patients had bone marrow uptake with a score of 4, which was classified as positive; the remaining 7 patients had bone marrow intensity with a score of 3 (in 6 patients) and a score of 2 (in 1 patient). The individual SUV_{max} of bone marrow for both ^{68}Ga-pentixafor PET/CT and ^{18}F-FDG PET/CT are shown in Supplemental Table 1 (supplemental materials are available at http://jnm.snmjournals.org).

In comparisons of ^{68}Ga-pentixafor and ^{18}F-FDG, 10 patients had visually higher uptake in the bone marrow on ^{68}Ga-pentixafor PET than on ^{18}F-FDG PET (example in Fig. 1A); in 6 patients, the intensities of the bone marrow uptake on ^{68}Ga-pentixafor PET and ^{18}F-FDG PET were comparable; and in only 1 patient was ^{18}F-FDG

TABLE 2
Diagnostic Performance of ^{68}Ga-Pentixafor and ^{18}F-FDG PET/CT

Parameter	^{68}Ga-pentixafor		^{18}F-FDG		*P*
	No. of patients	% of patients	No. of patients	% of patients	
Patients with positive PET results*	17/17	100	10/17	58.8	0.023*
Bone marrow involvement	16/17	94.1	10/17	58.8	0.077
Lymph node involvement	13/17	76.5	2/17	11.8	0.003*
Paramedullary involvement	3/17	17.6	0/17	0	0.248
CNS involvement	1/17	5.9	0/17	0	1.0

*Difference in rates of positive results between ^{68}Ga-pentixafor and ^{18}F-FDG was significant.

CNS = central nervous system.

Positive results for ^{68}Ga-pentixafor were defined by uptake > liver; positive results for ^{18}F-FDG were defined by uptake with score of ≥4 (5-point scale).

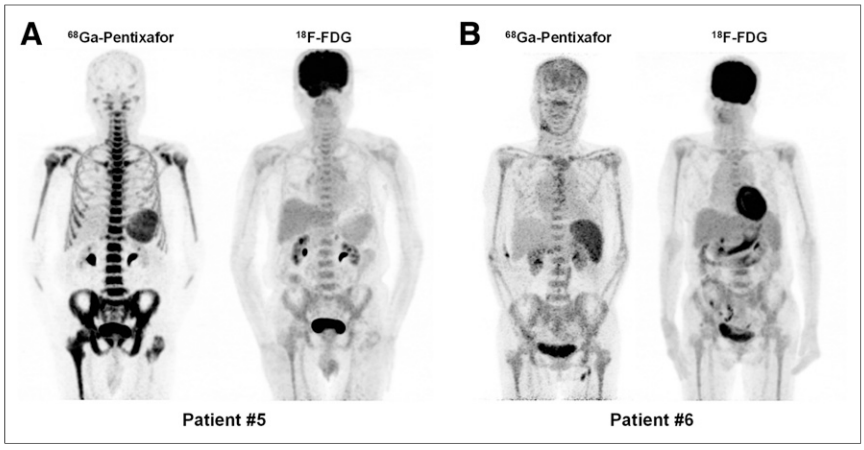

FIGURE 1. Examples of ^{68}Ga-pentixafor PET and ^{18}F-FDG PET in patients with WM/LPL. (A) Patient 5 had relapse of WM (IgM κ), had ISS-WM score of 4, and was classified as being at high risk. ^{68}Ga-pentixafor showed intense radioactivity that was much higher than that shown by ^{18}F-FDG in bone marrow (score of 3). (B) Patient 6 had WM (IgM κ) and secondary amyloidosis in myocardium, had ISS-WM score of 3, and was classified as being at high risk. Intensities of ^{68}Ga-pentixafor uptake and ^{18}F-FDG uptake in bone marrow were comparable, but bone marrow involvement was more extensive with ^{68}Ga-pentixafor than with ^{18}F-FDG. Additional bone marrow disease was detected in craniofacial bones, ulna, radius, carpal bones, and metacarpal bones with ^{68}Ga-pentixafor. Submandibular, retroperitoneal, and inguinal lymph nodes had positive results on ^{68}Ga-pentixafor PET, but these lymph nodes were not ^{18}F-FDG–avid.

uptake in the bone marrow higher than that of ^{68}Ga-pentixafor. Regarding the extent of bone marrow involvement, ^{68}Ga-pentixafor PET demonstrated more extensive bone marrow disease in 8 patients than ^{18}F-FDG PET (example in Fig. 1B), specifically when the involvement of the craniofacial bones (in 7 patients) and distal upper extremity bones (in 2 patients) was visualized. The bone marrow involvement mainly appeared as diffuse bone marrow patterns with homogeneous radioactivity throughout the axial and appendicular skeletons; moreover, additional focal bone marrow lesions were detected by ^{68}Ga-pentixafor PET in 3 patients (example in Figure 2A). Among these 3 patients, only 1 was found to have focal lesions by ^{18}F-FDG PET. No bone destruction was found in the coregistered CT. Despite the superiority of ^{68}Ga-pentixafor over ^{18}F-FDG in detecting bone marrow involvement, we did not find significant correlations between the SUV of bone marrow in baseline ^{68}Ga-pentixafor PET and the laboratory results, including hemoglobin, serum IgM, M protein, β_2-microglobulin, and serum free light chain levels and the proportion of lymphoplasmacytic cells in bone marrow biopsies.

Lymph Node Involvement. On ^{68}Ga-pentixafor PET/CT, 13 of 17 patients (76.5%) had positive lymph nodes (examples in Fig. 2), including neck (9 patients), axilla (7 patients), mediastinum (3 patients), internal mammary (1 patient), hepatoduodenal (11 patients), paraaortic (11 patients), iliac (7 patients), inguinal (7 patients), and epitrochlear (1 patient) nodes. Eight patients had involvement in more than 5 lymph node regions. The maximum size of the positive node in each patient was 16.5 ± 7.1 mm (range, 5–26 mm), with an SUV_{max} of 8.3 ± 3.9 (range, 4.0–18.8) (Supplemental Table 1). However, with ^{18}F-FDG PET/CT, only 2 patients were found to have mildly ^{18}F-FDG–avid lymph nodes (score, 3 or 4; SUV_{max}, 2.9); moreover, ^{68}Ga-pentixafor PET/CT detected more positive lymph nodes with higher radioactivity in these 2 patients than ^{18}F-FDG PET/CT. No lymph node involvement was detected in 4 patients with either ^{68}Ga-pentixafor PET/CT or ^{18}F-FDG PET/CT.

Paramedullary Involvement and Involvement of Other Organs. Paramedullary disease in 3 of 17 patients (17.6%) affected the soft tissues around the sternum, thoracic vertebrae, and presacral space. Among these 3 patients, 1 also had involvement in the thoracic nerve root and sacral nerve root (patient 4; Fig. 2B); this finding was confirmed by electromyography. ^{68}Ga-pentixafor PET/CT showed intense radioactivity in the paramedullary and nerve root regions; however, the intensity of ^{18}F-FDG uptake in the lesions was scored as 2 or 3—scores that are much lower than those for ^{68}Ga-pentixafor uptake. The patient with thoracic and sacral nerve root involvement also had central nervous system disease (Bing–Neel syndrome). ^{68}Ga-pentixafor PET/CT in this patient showed markedly increased radioactivity that was not ^{18}F-FDG–avid in the bilateral choroid plexus, and the abnormal ^{68}Ga-pentixafor uptake in the choroid plexus returned to normal after 6 cycles of chemotherapy. Another 3 patients were found to have splenomegaly, with ^{18}F-FDG uptake that was scored as 3 or 4.

Follow-Up PET/CT After Chemotherapy

Four patients underwent follow-up ^{68}Ga-pentixafor and ^{18}F-FDG PET/CT after 6 or 7 cycles of chemotherapy. The intervals between the last cycle of chemotherapy and the PET/CT study were 2 wk to 3 mo. According to the consensus response criteria adopted at the Sixth International Workshop on Waldenström Macroglobulinemia (*15*), 2 patients with a complete response or a very good partial response showed complete remission of the bone marrow and extramedullary involvement with both ^{68}Ga-pentixafor PET/CT and ^{18}F-FDG PET/CT (example in Fig. 3); another patient with a very good partial response had only several remnant CXCR4-positive axillary lymph nodes. The remaining patient who had a partial serological response showed a marked reduction of bone marrow uptake with ^{68}Ga-pentixafor and ^{18}F-FDG (^{18}F-FDG: score of 2; ^{68}Ga-pentixafor: mild uptake) and complete resolution of the involved lymph nodes.

DISCUSSION

The diagnosis of diffuse bone marrow involvement of lymphoma with ^{18}F-FDG PET/CT has always been a clinical dilemma for nuclear medicine physicians. Diffusely increased bone marrow ^{18}F-FDG uptake is commonly observed in patients with anemia or reactive hyperplasia or those treated with growth factors rather than patients with lymphomatous bone marrow involvement (*16,17*). Meanwhile, ^{18}F-FDG PET/CT can miss low-volume involvement (typically <20% of the marrow) and low-grade lymphoma in bone marrow (*16*). WM/LPL is an indolent lymphoma that primarily involves the bone marrow, and anemia is observed in more than 1 of 3 WM/LPL patients; the latter finding is partly related to B-cell infiltration in the bone marrow, blood loss, IgM-associated hemolysis, low erythropoietin levels, or concomitant iron deficiency (*18,19*). Therefore, bone marrow ^{18}F-FDG uptake in WM/LPL patients is complicated.

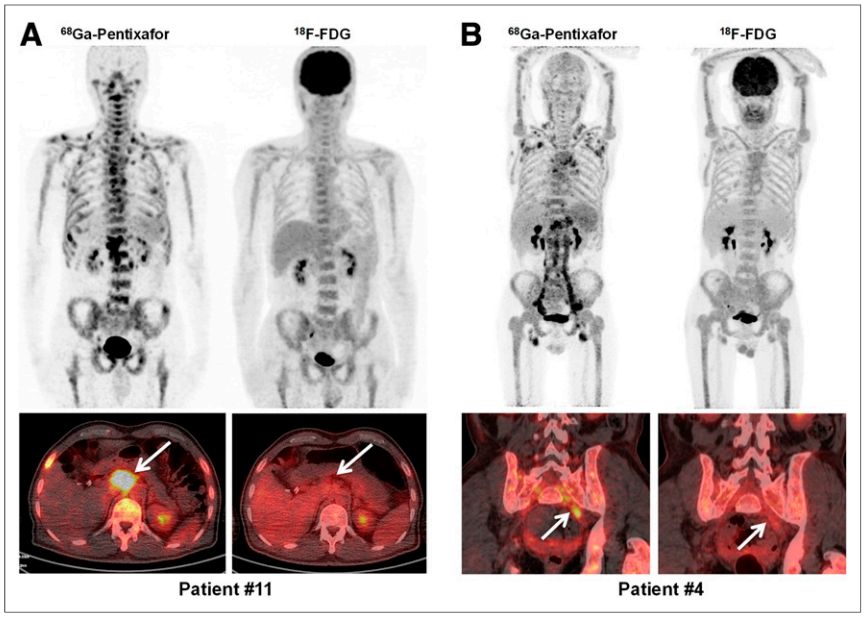

FIGURE 2. Examples of ^{68}Ga-pentixafor and ^{18}F-FDG PET/CT in WM/LPL patients with focal bone marrow lesions, positive lymph nodes, and other involvements. (A) Patient 11 had WM (IgM λ), had ISS-WM score of 2, and was classified as being at indeterminate risk. ^{68}Ga-pentixafor showed intense radioactivity in bone marrow, with multiple focal lesions and CXCR4-positive lymph nodes (arrow). ^{18}F-FDG activity (score of 4) was homogeneously distributed in bone marrow, and lymph nodes were not ^{18}F-FDG–avid (arrow). (B) Patient 4 had WM (IgM κ) and Bing–Neel syndrome, had ISS-WM score of 2, and was classified as being at indeterminate risk. Multiple CXCR4-positive lymph nodes were detected in neck, axilla, and hepatoduodenal, retroperitoneal, iliac, and inguinal regions, and most of these lymph nodes were missed with ^{18}F-FDG PET. Involved left iliac nerve root (arrow) was CXCR4-positive but was not ^{18}F-FDG–avid.

In the present study, 14 of 17 patients (82.4%) had anemia (median hemoglobin level of 89.5 g/L), which might have contributed to the bone marrow activity. In contrast, the percentage of lymphoplasmacytic cells that infiltrated the bone marrow was relatively low; more than 80% of the patients had less than 20% marrow infiltration. These factors and, of course, the indolent nature explained the low sensitivity of ^{18}F-FDG for detecting bone marrow involvement in WM/LPL patients. In the present study, we explored whether ^{68}Ga-pentixafor, a PET agent for the in vivo mapping of CXCR4 expression, is superior to ^{18}F-FDG for diagnosing WM/LPL because there is a high level of CXCR4 expression in the B cells of WM/LPL patients (*8,9*). We found that ^{68}Ga-pentixafor had a higher sensitivity for detecting bone marrow involvement than ^{18}F-FDG (94.1% vs. 58.8%; $P = 0.077$), although the difference was not significant, probably because of the small sample size. The intensity of radioactivity and the extent of bone marrow involvement shown on PET/CT and the ability to detect focal bone marrow lesions with ^{68}Ga-pentixafor were also advantages over ^{18}F-FDG.

Lymphadenopathy has been reported to occur in approximately 20%–25% of patients with WM/LPL (*18,20*). In the present study, the rate of lymph node involvement found with ^{18}F-FDG PET/CT was consistent with that reported in the literature (rate of positive results, 11.8%; SUV_{max}, 2.9). Surprisingly, we noted that most of the lymph node involvement found by ^{68}Ga-pentixafor PET was missed by ^{18}F-FDG PET. The rate of positive results for lymph node involvement was significantly higher with ^{68}Ga-pentixafor than with ^{18}F-FDG (76.5% vs. 11.8%; $P = 0.003$) in the recruited WM/LPL patients. Most of the involved lymph nodes showed intense uptake of ^{68}Ga-pentixafor (mean SUV_{max}, 8.3; range, 4.0–18.8). The most commonly involved lymph nodes were the hepatoduodenal (19%), paraaortic (19%), cervical (16%), axillary (12%), iliac (12%), and inguinal (12%) nodes. Because previous data on lymphadenopathy in WM/LPL were usually based on CT criteria, we believe that the true percentage of lymph node involvement in WM/LPL might be much higher than the current data suggest, on the basis of the findings of ^{68}Ga-pentixafor PET/CT. Similarly, paramedullary involvement and central nervous system disease showed intense radioactivity on ^{68}Ga-pentixafor PET, but the results were negative on ^{18}F-FDG PET. These results imply that ^{68}Ga-pentixafor might be a very promising imaging agent for the diagnosis and staging of WM/LPL.

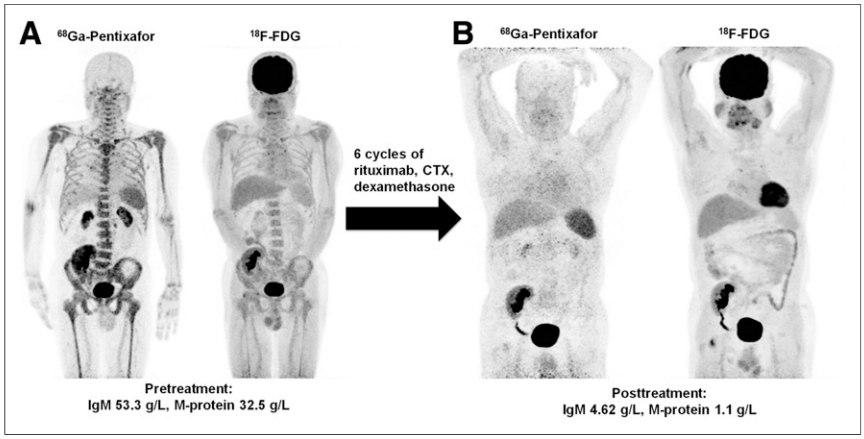

FIGURE 3. Patient 12 had WM (IgM κ), had ISS-WM score of 2, and was classified as being at indeterminate risk. (A) Pretreatment ^{68}Ga-pentixafor and ^{18}F-FDG PET/CT showed diffuse involvement in bone marrow. There was also lymph node involvement in neck, mediastinum, and hepatoduodenal, retroperitoneal, and inguinal regions, as depicted on ^{68}Ga-pentixafor PET/CT. (B) Posttreatment ^{68}Ga-pentixafor and ^{18}F-FDG PET/CT performed 2 wk after completion of 6 cycles of chemotherapy (cyclophosphamide, rituximab, dexamethasone [DRC]) showed complete remission of bone marrow and lymph node disease on both ^{68}Ga-pentixafor PET/CT and ^{18}F-FDG PET/CT. Serum IgM and M protein levels were markedly decreased compared with those at baseline.

There might be some limitations of ^{68}Ga-pentixafor. First, apart from CXCR4-positive tumor cell infiltration, other activated inflammatory cells in the bone marrow with upregulated CXCR4 expression might also cause increased bone marrow uptake (*21–23*). Therefore, the specificity of diagnosing diffuse bone marrow involvement might be

hampered in the differentiation of different diseases in future studies. Second, because of the lack of histologic verification of lymph node involvement in the present study, false-positive results for lymph nodes might be caused by inflammation—especially for nodes with moderate ^{68}Ga-pentixafor uptake and in patients with a limited number of positive nodes. Third, the incidence of splenic involvement caused by the infiltration of clonal cells was reported to be 20%–25% in WM/LPL (*18,20*). Consistent with the literature, splenomegaly with mildly increased ^{18}F-FDG uptake (uptake > liver) was noted in 17.6% of patients in the present study. However, establishing an interpretation criterion to define the high spleen uptake of ^{68}Ga-pentixafor might be difficult because there is considerable physiologic uptake in the normal spleen. Finally, in the 4 patients who underwent follow-up PET/CT after chemotherapy, we found an almost complete response on both ^{68}Ga-pentixafor PET/CT and ^{18}F-FDG PET/CT. However, the surface expression of CXCR4 in tumor cells is a dynamic process that is influenced by therapeutic interventions. Chemotherapy may induce CXCR4 downregulation in multiple myeloma, diffuse large B-cell lymphoma, and acute lymphoblastic leukemia (*24,25*). If this is also the case in WM/LPL, images must be interpreted with caution to avoid misinterpretation of the tumor response. Moreover, it is important to further investigate the time- and dose-dependent influence of each chemotherapeutic drug on CXCR4 expression in different tumors.

CONCLUSION

In the present study, we found that ^{68}Ga-pentixafor PET/CT had a higher rate of positive results than ^{18}F-FDG PET/CT for detecting tumor involvement of the bone marrow, lymph nodes, and other extramedullary organs in WM/LPL patients. Further studies are warranted to clarify the role of ^{68}Ga-pentixafor in staging, assessing the response to therapy, and predicting the prognosis for WM/LPL patients.

DISCLOSURE

This work was supported by the National Natural Science Foundation of China (81701741); the CAMS Initiative for Innovative Medicine (CAMS-I2M, 2017-I2M-3-001); and the Research Fund for International Young Scientists of PUMC, the Fundamental Research Funds for the Central Universities (2017320004). No other potential conflict of interest relevant to this article was reported.

KEY POINTS

QUESTION: Is ^{68}Ga-pentixafor PET/CT superior to ^{18}F-FDG PET/CT for detecting tumor involvement in Waldenström macroglobulinemia/lymphoplasmacytic lymphoma (WM/LPL)?

PERTINENT FINDINGS: In our prospective cohort study of 17 patients with WM/LPL, ^{68}Ga-pentixafor PET/CT had a higher rate of positive results than ^{18}F-FDG PET/CT for detecting bone marrow involvement, lymph node involvement, and other extramedullary involvement.

IMPLICATIONS FOR PATIENT CARE: ^{68}Ga-pentixafor PET/CT might be a promising tool for the assessment of WM/LPL.

REFERENCES

1. Cheson BD, Fisher RI, Barrington SF, Cavalli F, Schwartz LH, Lister TA. Recommendations for initial evaluation, staging, and response assessment of Hodgkin and non-Hodgkin lymphoma: the Lugano classification. *J Clin Oncol.* 2014;32:3059–3068.
2. Banwait R, O'Regan K, Campigotto F, et al. The role of ^{18}F-FDG PET/CT imaging in Waldenstrom macroglobulinemia. *Am J Hematol.* 2011;86:567–572.
3. Teicher BA, Fricker SP. CXCL12 (SDF-1)/CXCR4 pathway in cancer. *Clin Cancer Res.* 2010;16:2927–2931.
4. Philipp-Abbrederis K, Herrmann K, Knop S, et al. In vivo molecular imaging of chemokine receptor CXCR4 expression in patients with advanced multiple myeloma. *EMBO Mol Med.* 2015;7:477–487.
5. Wester HJ, Keller U, Schottelius M, et al. Disclosing the CXCR4 expression in lymphoproliferative diseases by targeted molecular imaging. *Theranostics.* 2015; 5:618–630.
6. Herhaus P, Habringer S, Philipp-Abbrederis K, et al. Targeted positron emission tomography imaging of CXCR4 expression in patients with acute myeloid leukemia. *Haematologica.* 2016;101:932–940.
7. Lapa C, Schreder M, Schirbel A, et al. [^{68}Ga]Pentixafor-PET/CT for imaging of chemokine receptor CXCR4 expression in multiple myeloma: comparison to [^{18}F]FDG and laboratory values. *Theranostics.* 2017;7:205–212.
8. Ngo HT, Leleu X, Lee J, et al. SDF-1/CXCR4 and VLA-4 interaction regulates homing in Waldenstrom macroglobulinemia. *Blood.* 2008;112:150–158.
9. Hunter ZR, Yang G, Xu L, Liu X, Castillo JJ, Treon SP. Genomics, signaling, and treatment of Waldenstrom macroglobulinemia. *J Clin Oncol.* 2017;35:994–1001.
10. Luo Y, Pan Q, Feng J, Cao X, Li F. Chemokine receptor CXCR4-targeted PET/CT with ^{68}Ga-Pentixafor shows superiority to ^{18}F-FDG in a patient with Waldenstrom macroglobulinemia. *Clin Nucl Med.* 2018;43:548–550.
11. Nanni C, Versari A, Chauvie S, et al. Interpretation criteria for FDG PET/CT in multiple myeloma (IMPeTUs): final results—IMPeTUs (Italian myeloma criteria for PET USe). *Eur J Nucl Med Mol Imaging.* 2018;45:712–719.
12. Morel P, Duhamel A, Gobbi P, et al. International Prognostic Scoring System for Waldenstrom Macroglobulinemia. *Blood.* 2009;113:4163–4170.
13. Treon SP, Xu L, Yang G, et al. MYD88 L265P somatic mutation in Waldenstrom's macroglobulinemia. *N Engl J Med.* 2012;367:826–833.
14. Hunter ZR, Xu L, Yang G, et al. The genomic landscape of Waldenstrom macroglobulinemia is characterized by highly recurring MYD88 and WHIM-like CXCR4 mutations, and small somatic deletions associated with B-cell lymphomagenesis. *Blood.* 2014;123:1637–1646.
15. Treon SP. How I treat Waldenstrom macroglobulinemia. *Blood.* 2015;126:721–732.
16. Barrington SF, Mikhaeel NG, Kostakoglu L, et al. Role of imaging in the staging and response assessment of lymphoma: consensus of the International Conference on Malignant Lymphomas Imaging Working Group. *J Clin Oncol.* 2014;32: 3048–3058.
17. Adams HJ, Nievelstein RA, Kwee TC. Opportunities and limitations of bone marrow biopsy and bone marrow FDG-PET in lymphoma. *Blood Rev.* 2015;29:417–425.
18. Kapoor P, Paludo J, Vallumsetla N, Greipp PR. Waldenstrom macroglobulinemia: what a hematologist needs to know. *Blood Rev.* 2015;29:301–319.
19. Mazzucchelli M, Frustaci AM, Deodato M, Cairoli R, Tedeschi A. Waldenstrom's macroglobulinemia: an update. *Mediterr J Hematol Infect Dis.* 2018;10:e2018004.
20. Ghobrial IM, Gertz MA, Fonseca R. Waldenstrom macroglobulinaemia. *Lancet Oncol.* 2003;4:679–685.
21. Cytawa W, Kircher S, Schirbel A, et al. Chemokine receptor 4 expression in primary Sjogren's syndrome. *Clin Nucl Med.* 2018;43:835–836.
22. Derlin T, Gueler F, Brasen JH, et al. Integrating MRI and chemokine receptor CXCR4-targeted PET for detection of leukocyte infiltration in complicated urinary tract infections after kidney transplantation. *J Nucl Med.* 2017;58:1831–1837.
23. Margaritopoulos GA, Antoniou KM, Lasithiotaki I, Proklou A, Soufla G, Siafakas NM. Expression of SDF-1/CXCR4 axis in bone marrow mesenchymal stem cells derived from rheumatoid arthritis-usual interstitial pneumonia. *Clin Exp Rheumatol.* 2013;31:610–611.
24. Lapa C, Herrmann K, Schirbel A, et al. CXCR4-directed endoradiotherapy induces high response rates in extramedullary relapsed multiple myeloma. *Theranostics.* 2017;7:1589–1597.
25. Lapa C, Luckerath K, Kircher S, et al. Potential influence of concomitant chemotherapy on CXCR4 expression in receptor directed endoradiotherapy. *Br J Haematol.* 2019;184:440–443.